NEW DEVELOPMENTS IN TARGET DETECTION IN HYPERSPECTRAL IMAGERY USING SPECTRAL METRICS AND SPECTRA EXTRACTION

Stefan Robila
Center for Imaging and Optics
Department of Computer Science
Montclair State University
Richardson Hall 301
Upper Montclair, NJ 07043
robilas@mail.montclair.edu

ABSTRACT

An important problem in processing multispectral / hyperspectral imagery consists in the design of methods for the detection of targets. In this paper we investigate a class of detection filters based on band and spectral selection. Band selection (band screening) refers to searching for the spectral bands that would yield the largest separation between target and background. Spectral selection (spectral screening) is a technique used in reducing the multispectral / hyperspectral data to a representative subset of spectra. The subset is formed such that any two spectra in it are dissimilar and, for any spectrum in the original image cube, there is a similar spectrum in the subset. Spectral screening is performed in a sequential manner, at each step, the subset being increased with a spectrum dissimilar from all the spectra already selected.
We modified the spectral screening algorithm such that at the selection step the spectrum with the largest distance from the set is selected. While not introducing additional computational complexity, the Maximum Spectral Screening (MSS) algorithm ensures that the overlap among the representatives is minimized. The detection filters were obtained as the classification projector matrices based on the spectral subset. The developed algorithms were tested on HYDICE hyperspectral data using the spectral angle and the spectral information divergence. The results indicate that regular MSS outperforms band selection followed by MSS, both classes outperforming regular spectral screening.

INTRODUCTION

In remote sensing, one of the most dynamic and growing areas is constituted by hyperspectral data processing. Hyperspectral images are based on recording the scene's reflected light in bands associated to narrow intervals of spectrum wavelengths (see Figure 1). Each element from the image (pixel) is associated with a certain area of the surveyed scene and with its spectral response (see Figure 2). Grouping spectral images over several wavelength intervals for the same scene results in *multispectral* (in case of few wide spectral bands) or *hyperspectral* (in case of many narrow spectral bands) *images* (Lillesand, 2000). Usually, passive hyperspectral sensors cover wavelengths from the visible range (0.4μm-0.7μm) to the middle infrared range (2.4μm) (Richards, 1999). The Figures 1 and 2 show parts of hyperspectral data collected in Montclair, NJ, in Summer 2005 with a Surface Optics SOC hyperspectral camera able to distinguish among 120 spectral bands within the 400nm to 900nm. Note in Figure 1 the difference between the top row of grayscale images (corresponding to blue, green and red bands) and the bottom row (with bands affiliated to near-infrared bands). Parts of the vegetation pot start displaying different reflectances, due to the difference in composition (fake vs. real vegetation).

Compared to regular imagery, hyperspectral data have the advantage of being able to distinguish among minute differences in material composition and color by using the rich spectral information. This richness becomes clear when we plot the pixel vectors. Figure 3a shows a hyperspectral image band collected with the HYDICE sensor (Hydice 1995). Eight rows of panels are indicated by marks of various colors in the image, with each row containing three panels of 1mx1m, 2mx2m and 3mx3m, respectively, made of the same material. While the panels are hard to distinguish within most of the image bands, the plot of their pixel vectors displays significant differences for each. A processing tool that is able to distinguish the materials based on spectral dissimilarities will provide significantly better results than any analysis of the individual images.

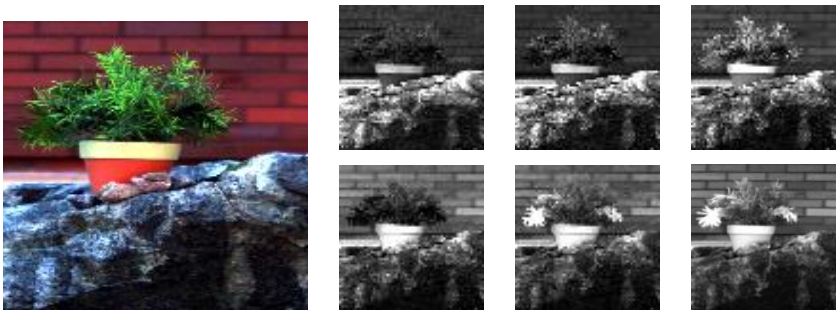

(a) (b)

Figure 1. Hyperspectral images are formed by combining a large number of narrow spectrum bands. a) color composite image b) spectral bands ranging from visible (blue, green, red – top row) to near infrared (bottom row).

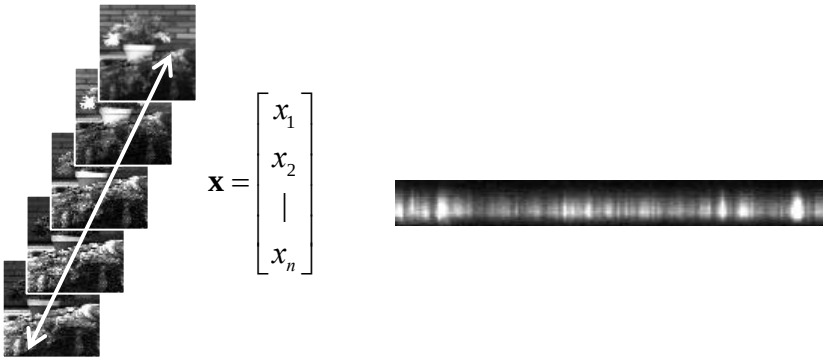

(a) (b)

Figure 2. a) Pixel vectors are formed of the pixel values for the same coordinates. b) A vertical slice through the data cube displaying variations among spectra.

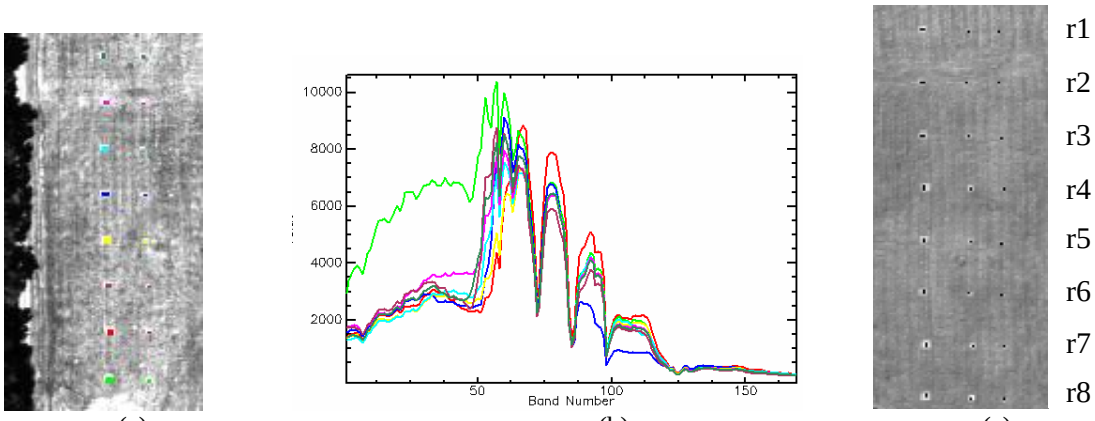

(a) (b) (c)

Figure 3. a) HYDICE data displaying rows of panels marked by squares, b) Average spectra for the eight panel categories in the scene c) Exact location of the pixels used for desired target signatures.

These characteristics have allowed hyperspectral data to be successfully employed in varied fields including agricultural monitoring, mineral identification, military, emergency planning, and medical and industrial imaging [Bannon 2004].

At the basis of multispectral / hyperspectral data processing lays the idea of spectra separability. If a material spectrum is easily separable from the background, then the material will be easily detected in the image. If two adjoining materials have significantly dissimilar spectra, then the edge between them will also be easily detected.

Unfortunately, clear separability cannot be easily achieved. Each spectrum is formed of tens to hundreds of values collected within narrow adjacent wavelength intervals and often exposes strong local correlation [Robila 2003]. Solutions to target separability are often found in the literature. They range from the use of spectral distances (such as spectral angle, euclidean distance, etc.)[Kruse 1993, Robila 2005b], to preprocessing of the bands (through feature extraction) and data projections (such as orthogonal subspace projection) [Du 2004].

In this paper we present a hybrid class of methods for target detection based on *band and spectra separability*. The unsupervised algorithms generate first a set of bands that increase the separability of the target from the background. Next, with the target spectra as origin, the algorithms generate a set of spectra that are dissimilar from each other in terms of a spectral distance measure. The spectral subset is obtained through a modified selection algorithm known as *spectral screening* [Achalakul 2003], or *exemplar selection* [Plaza 2004]. In spectral screening, the subset is built gradually with each newly added spectra being dissimilar from the ones already selected. If we eliminate from the subset the desired target spectra we end up with a collection of signatures that characterize the background (with respect to the spectra). The spectral subset is thus used to build a target detection filter that, using orthogonal subspace projection will identify pixels that closely match the selected spectra.

SPECTRAL DISTANCES

Spectral Angle (SA)

Given two vectors of the same dimension **x** and **y**, the *spectral angle* is defined as the arccosine of their dot product [Kruse 1993]:

$$SA(\mathbf{x},\mathbf{y}) = \arccos\left(\frac{\langle \mathbf{x},\mathbf{y}\rangle}{\|\mathbf{x}\|_2 \|\mathbf{y}\|_2}\right) \tag{1}$$

where <.,.> represents the dot product of the vectors and ||.|| the Euclidean norm.

When the pixel vectors represent reflectance values, two spectra with zero-angle would correspond to the same material under different illumination conditions (poor illumination leads to shorter segments, strong illumination will yield longer segments) [Robila 2005a]. The spectral angle was used as a method for mapping the spectral similarity of image spectra to the reference spectra [Carvahlo 2000, Chang 2000] and has been implemented is most of the widely used remote sensing software packages.

An important attribute for the spectral angle is that its values fall within a well-defined interval. In the case of reflectance values, since the pixels are all positively defined, the interval for the spectral angle is between 0 and $\pi/2$ irrespective of the amplitude of the various bands. This is important for algorithms that need to rely on threshold values for distance among spectra, since this threshold can be set without prior knowledge of the particular scene.

Spectral Information Divergence (SID)

Given two *n*-dimensional vectors **x** and **y**, the *spectral information divergence* is defined as [Du 2004]:

$$SID(\mathbf{x},\mathbf{y}) = \left\langle \frac{\mathbf{x}}{sum(\mathbf{x})} - \frac{\mathbf{y}}{sum(\mathbf{y})}, \log\left(\frac{\mathbf{x}}{sum(\mathbf{x})}\right) - \log\left(\frac{\mathbf{y}}{sum(\mathbf{y})}\right) \right\rangle \tag{2}$$

where the *sum*(**.**) function refers to the sum of the values composing the vectors **x**.

SID is derived from the Kullback-Leibler information measure:

$$SID(\mathbf{x},\mathbf{y}) = D(\mathbf{x}\,\|\,\mathbf{y}) + D(\mathbf{y}\,\|\,\mathbf{x}) \tag{3}$$

where $D(\mathbf{x}\|\mathbf{y})$ is defined as:

$$D(\mathbf{x}\,\|\,\mathbf{y}) = \sum_{i=\overline{1,n}} p_i \log\frac{p_i}{q_i} \tag{4}$$

and

$$(p_1, p_2, .., p_n) = \frac{\mathbf{x}}{sum(\mathbf{x})} \qquad (q_1, q_2, .., q_n) = \frac{\mathbf{y}}{sum(\mathbf{y})} \tag{5}$$

are probability mass functions associated with the two vectors.

The spectral information divergence has been shown to provide a relatively better quantification of similarity than the spectral angle. Unlike the spectral angle that is based on vector theory, SID is derived from information theory. Combinations of the SA and SID (by using tan and sin functions) have been proposed and shown to increase the accuracy over both measures [Du 2004].

BAND SCREENING

Given two spectra **x** and **y** with values over a set of spectra bands **B**, a spectral distance β the goal of band screening is to find the subset of bands $\mathbf{B_1}$ such that:

$$\beta(\mathbf{x}, \mathbf{y}, \mathbf{B_1}) = \max_{\mathbf{B_s} \subseteq \mathbf{B}} \beta(\mathbf{x}, \mathbf{y}, \mathbf{B_s}) \tag{6}$$

where by $\beta(\mathbf{x}, \mathbf{y}, \mathbf{B_s})$ we refer to the value of the distance measure β computed between the two vectors but taking into consideration only the bands included in the subset $\mathbf{B_s}$.

The goal in band screening is to find the subset of bands that maximize the distance between the two spectra [Keshava 2004]. While finding the optimum subset is always possible through exhaustive search, the complexity of such operation is prohibitive. Given a hyperspectral image of n bands, and assuming the B_1 can have any size (between 1 and 150), the number of band combinations to be tried is roughly equivalent to the number of possible mappings:

$$f : \{1, 2, 3, ..., n\} \rightarrow \{0, 1\} \tag{7}$$

This is because, each subset $\mathbf{B_s}$ of **B** can be seen as an n-uple of 0's and 1's where, for each position, one indicating that the corresponding band is in the subset and zero indicating the absence of the band. The above equation leads to 2^n possible mappings. Table 1 shows what the values amount to for various possible image sizes:

Table 1. Estimation of the number of subsets to be analyzed for optimum band selection, given images with the number of bands ranging from 25 to 200.

n	25	50	75	100	125	150	175	200
2^n	$3.4*10^7$	$1.1*10^{15}$	$3.8*10^{22}$	$1.3*10^{30}$	$4.3*10^{37}$	$1.4*10^{45}$	$4.8*10^{52}$	$1.6*10^{60}$

Recent news has revealed that Intel Corp has designed a teraflop computer able to perform 10^{12} operations every second [Intel 2007]. Assuming that the computation of the distance takes on average 10 cycles, this would mean that Intel's future machine would compute 10^{11} distance computations each second. For 200 bands, to perform exhaustive search will amounts to $1.6*10^{49}$ seconds (or $1.8*10^{44}$days, $5*10^{41}$ days) a number beyond anybody's ability to compute and provide relevant results. Even including cluster or grid computing, the problem may not be easier to tackle.

Given such somber predictions, the only approach to band screening would be the use of a sub-optimal algorithm. In [Keshava 2004], Keshava suggests such a method for the spectral angle. In that situation, the spectral angle between **x**, and **y**, and using the bands **B**, b was written as:

$$\cos\left(SA(\mathbf{x}, \mathbf{y}, [\mathbf{B}, b])\right) = \frac{< \mathbf{x}, \mathbf{y} >_{[\mathbf{B},b]}}{\sqrt{\|\mathbf{x}\|^2_{[\mathbf{B},b]}}\sqrt{\|\mathbf{y}\|^2_{[\mathbf{B},b]}}} = \frac{< \mathbf{x}, \mathbf{y} >_{[\mathbf{B}]}}{\sqrt{\|\mathbf{x}\|^2_{[\mathbf{B}]}}\sqrt{\|\mathbf{y}\|^2_{[\mathbf{B}]}}} \frac{1 + \frac{< \mathbf{x}, \mathbf{y} >_{[b]}}{< \mathbf{x}, \mathbf{y} >_{[\mathbf{B}]}}}{\sqrt{1 + \frac{\|\mathbf{x}\|^2_{[b]}}{\|\mathbf{x}\|^2_{[\mathbf{B}]}}}\sqrt{1 + \frac{\|\mathbf{y}\|^2_{[b]}}{\|\mathbf{y}\|^2_{[\mathbf{B}]}}}} = \cos(\mathbf{x}, \mathbf{y}, \mathbf{B}) \frac{1 + \frac{< \mathbf{x}, \mathbf{y} >_{[b]}}{< \mathbf{x}, \mathbf{y} >_{[\mathbf{B}]}}}{\sqrt{1 + \frac{\|\mathbf{x}\|^2_{[b]}}{\|\mathbf{x}\|^2_{[\mathbf{B}]}}}\sqrt{1 + \frac{\|\mathbf{y}\|^2_{[b]}}{\|\mathbf{y}\|^2_{[\mathbf{B}]}}}} \tag{8}$$

In this case, the band b will increase the spectral angle between the two spectra only if the second term is smaller than 1. The algorithms will exhaustively search through all the bands to find the one with the smallest value:

$$b_s = \arg\min_{b \notin \mathbf{B}} \frac{1 + \frac{< \mathbf{x}, \mathbf{y} >_{[b]}}{< \mathbf{x}, \mathbf{y} >_{[\mathbf{B}]}}}{\sqrt{1 + \frac{\|\mathbf{x}\|^2_{[b]}}{\|\mathbf{x}\|^2_{[\mathbf{B}]}}} \sqrt{1 + \frac{\|\mathbf{y}\|^2_{[b]}}{\|\mathbf{y}\|^2_{[\mathbf{B}]}}}} \tag{9}$$

The method is clearly not optimal since it corresponds to a localized search for optimal solution and no suboptimality property for the global problem was proven. However, experiments with synthetic and real hyperspectral data suggests that the resulting bands improve target separability [Keshava 2004]. In addition, when used for target detection based on spectra library, the algorithm is based on average distance rather than exact distance.

We expand this algorithm to cover any spectral distance. Given a set of spectra $\mathbf{t_1}$, $\mathbf{t_2}$, … corresponding to a target and a set of undesired background signatures $\mathbf{s_1}$, $\mathbf{s_2}$, … a set of already selected bands **B,** we will select the next band according to one of the two criteria:

SBminT: $$b_s = \arg\min_{b \notin \mathbf{B}} E[\beta(\mathbf{t}, E[\mathbf{t}], [\mathbf{B}, b]] \tag{10}$$

SBMaxBT: $$b_s = \arg\max_{b \notin \mathbf{B}} \left(E[\beta(\mathbf{s}, E[\mathbf{t}], [\mathbf{B}, b]] - E[\beta(\mathbf{t}, E[\mathbf{t}], [\mathbf{B}, b]] \right) \tag{11}$$

In *SBminT* we select the band as the one that minimizes the distance (on average) between the target spectra and the average target spectra (i.e. we encourage the "collapsing" of the target cluster). In SBMaxBT we select the band as the one that maximizes the difference between the average distances of the non-targets and targets compared to the average target spectra. In this case the goal is to increase the separability between the targets and non-targets.

In both cases, the band screening will stop when the quality measure is no longer improving (decreasing for Eq. 10, and increasing for Eq. 11).

SPECTRAL SCREENING

Given a spectral distance measure $d(.,.)$, and a threshold or error value β, we say that two spectra **x** and **y** are *similar* with respect to d and β if $d(\mathbf{x}, \mathbf{y}) \leq \beta$. The two spectra are *dissimilar* otherwise. Based on this characterization of similarity we proceed to describe a method that generates from the data a subset of dissimilar spectra. The number of selected spectra depends on the distance used and on the threshold β. As the value of β decreases, the number of spectra that are found to be similar also decreases, increasing in turn the subset size. Moreover, the number of selected spectra depends on the order they are processed.

Spectral screening was used for exemplar selection in [Bowles 1997]. The screened subset was then employed for endmember extraction for the linear mixing model [Plaza 2004]. The abundances for the spectra from the original data are obtained by computing and applying filter vectors to it [Bowles 2003]. An interesting modification of the spectral screening is described in [Bowles 2003]. In this case, once a similar spectrum is found in the subset, the process continues the search, until the 'most similar' one is found. The new algorithm is described as 'best fit', as compared to the original 'first fit'. Several other applications are encountered in the literature. In [Achalakul 2003], a non-weighted spectral screening process is employed to derive a distributed spectral screening algorithm. The data are split in smaller subcubes that are processed separately. A color-composite scheme is used to generate the final image out of the first few PCA bands. The authors suggest that the use of spectral screening allows a fast, if not real time processing and an emphasis of the targets. Complimentarily, in [Robila 2005a], spectral screening is employed prior to runs of ICA. The experiments suggest that apart from speedup, the screened subset is beneficial in separation of the target information.

A problem encountered when using spectral screening is related to the overlap of the similarity sets. Each spectrum from the original data is eliminated based to its similarity with one of the subset spectra. However, it is likely that the original spectrum be similar to more than one of the selected spectra. The association of one individual with several clusters could affect the results of any subsequent processing [Robila 2006]. Instead of

focusing on the best match between a data spectrum and the subset spectrum, we suggest analyzing the problem from the point of view of subset generation. In the original algorithm, at every iterative step, the next subset element is chosen as the first one found to be dissimilar to all the spectra already included in the subset. To reduce the possibility of overlaps, we suggest a modification in the choice of the next candidate for the screened subset. Here, instead of randomly picking the next dissimilar sample, we will choose the one that is the farthest away from all the already selected spectra. In other words, the algorithm chooses at each step, the most dissimilar spectra left. In case the subset contains only one spectrum $\mathbf{x_1}$, the farthest away will be easily identified as:

$$\bar{\mathbf{x}} = \arg(\max_{\mathbf{x}}(d(\mathbf{x}, \mathbf{x_1})) \tag{12}$$

In case several spectra ($\mathbf{x_1}$, $\mathbf{x_2}$, …,$\mathbf{x_k}$) are already selected in the subset, we find the most distant spectra as the one with the largest value for the product of the distances from it to $\mathbf{x_1}$, $\mathbf{x_2}$, …,$\mathbf{x_k}$ respectively:

$$\bar{\mathbf{x}} = \arg(\max_{\mathbf{x}}(\prod_{i=1}^{k} d(\mathbf{x}, \mathbf{x_i})) \tag{13}$$

The choice for the next spectra stays at the basis of the Maximum Spectral Screening algorithm presented in Figure 4. A *cumulative_dist* attribute is associated to each of the spectra in the original image cube *S* (line2). The attribute will be used to compute the product of the distances between the spectrum and the samples selected in S_I. At each iterative step, all the spectra left in S that are similar (according to *d* and β) to the last sample $\bar{\mathbf{x}}$ chosen for S_I are eliminated (lines 9-10). For each dissimilar distance, the cumulative distance is updated by multiplying it with the distance between them and $\bar{\mathbf{x}}$ (line 12). The sample with the maximum cumulative distance is selected to be included in S_I and eliminated from *S*. The algorithm terminates when all the spectra in S are eliminated. A full analysis of the MSS is described in [Robila 2006].

```
1     Let S= set of all spectra
2     cumulative_dist(x)=1, for all x in S
3     Let S_I=∅

      Initial Step:
4     Select x ∈S
5     S=S-{ x }
6     S_I={ x }

      Iterative Step:
7     While S is not empty
8           For all x in S
9                 If d(x, x )<β then
10                      S = S - {x}
11                Else
12                      cumulative_dist(x)= cumulative_dist(x)*d(x, x )
            End (for)
13          x = arg{max_{x∈S}[cumulative_dist(x)]}
14          S_I=S_I∪{ x }
15          S=S-{ x }
      End (while)
```

Figure 4. Maximum Spectral Screening (MSS) Algorithm

EXPERIMENTAL RESULTS

To investigate the usefulness of band and spectral screening we have devised a class of target detection algorithms described in Figure 5. For each target, the average target spectra is computed and used to find the subset of bands that optimize the separation. The resulting bands are employed in spectral screening to yield a spectral subset. The various resulting detection algorithms are summarized in Table 2. Note that in all cases, the Maximum Spectral Screening (MSS) algorithm is used. For an extensive comparison between MSS, spectral screening and the minimum spectral screening algorithm (a variation that selects the 'closest spectra') see [Robila 2006]**.**

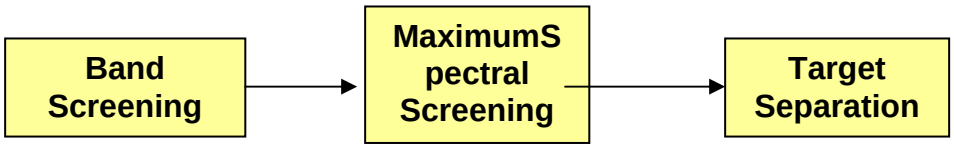

Figure 5. Diagram of the detection algorithms

Table 2. Band Screened/ Maximum Spectral Screened Algorithms

Algorithm	Band Selection	Spectral Distance
SBMinT- SA	SBMinT	SA
SBMinT- SID	SBMinT	SID
SBMaxBT- SA	SBMaxBT	SA
SBMaxBT- SID	SBMaxBT	SID
MSS-SA	-	SA
MSS-SID	-	SID

Note that the final step is done through orthogonal subspace projection. Given $\mathbf{s_0}$ the target spectrum, and $\mathbf{s_1}$, $\mathbf{s_2}$, ...,$\mathbf{s_m}$ a set of background (or undesired) spectra the OSP detection filter for $\mathbf{s_0}$ is defined as [Harsanyi 1994]:

$$\mathbf{P}_{\mathbf{s}_0} = \mathbf{s}_0\mathbf{P}_{\mathbf{U}}^{\perp}. \tag{14}$$

where $\mathbf{U} = [\mathbf{s_1}\ \mathbf{s_2}\ldots\mathbf{s_m}]$ the matrix formed by having the spectra $\mathbf{s_1}$, $\mathbf{s_2}$,…,$\mathbf{s_m}$ as columns and $\mathbf{P}_{\mathbf{U}}^{\perp}$ is the undesired target signature annihilator [Ren 2000a, Ren 2003]:

$$\mathbf{P}_{\mathbf{U}}^{\perp} = \mathbf{I} - \mathbf{U}\mathbf{U}^{\#}. \tag{15}$$

and $\mathbf{U}^{\#}$ is the pseudoinverse of $\mathbf{U}$:

$$\mathbf{U}^{\#} = (\mathbf{U}^{\mathrm{T}}\mathbf{U})^{-1}\mathbf{U}^{\mathrm{T}}. \tag{16}$$

The OSP filter would then be applied to each of the image spectra $\mathbf{x}$:

$$\mathbf{P}_{\mathbf{s}_0}\mathbf{x} = \mathbf{s}_0\mathbf{P}_{\mathbf{U}}^{\perp}\mathbf{x}. \tag{17}$$

The process above can be seen as one that eliminates the undesired target spectra. We note that the above equations hold for a spectral subset of relatively small size. When the number of background spectra surpasses the number of bands, then the matrix $(\mathbf{U}^{\mathbf{T}}\mathbf{U})^{-1}$ can no longer be computed. However, it can be safely assumed that the number of undesired spectra is small compared to the number of bands. Applying the classifier from equation (17) and to the spectra in the original data we get a detection image **I** for the target $\mathbf{s_0}$. The result is normalized to the [0,1] interval by subtracting its minimum and dividing by the difference between the maximum and minimum in the image [Ren 2000b]:

$$\mathbf{I}' = \frac{\mathbf{I} - \min_{\mathbf{I}}}{\max_{\mathbf{I}} - \min_{\mathbf{I}}} \quad . \tag{18}$$

The normalized abundance fractions are used with a threshold fraction α. If the pixel value is larger than α the pixel is labeled as target, otherwise it is labeled as background. Additional considerations for the use of OSP or KOSP (kernel orthogonal subspace projection) can be found in [Kwon 2006].

The experiments are using a Hyperspectral Digital Collection Experiment (HYDICE) image provided by the Spectral Information Technology Application Center. The image, with a size of 175 x 75 pixels was extracted from the Radiance I set [Hydice 1995]. Following the elimination of the water absorption and artifact corrupted bands, 166 bands were selected for processing. The scene contains 24 panels centrally located in the image (see Fig. 3). The panels are grouped in eight rows of three panels. Each row contains panels of the same material and of sizes 3m x 3m, 2m x 2m, and 1m x 1m (in decreasing order from left to right). Given the reported spatial resolution of 0.75m, it is highly probable that most if not all the pixels are mixed. Fig. 3b shows the location of each of the panels. The rows are labeled with r1 through r8 in top to bottom order. For each row, we selected four pixels that were averaged to compute the target spectra. The dark pixels in the image correspond to pixel locations of each of the spectra extracted. Fig 3a presents the plot of the average spectra for each of the eight targets. Note that the spectra plots indicate a high level of similarity among the data.

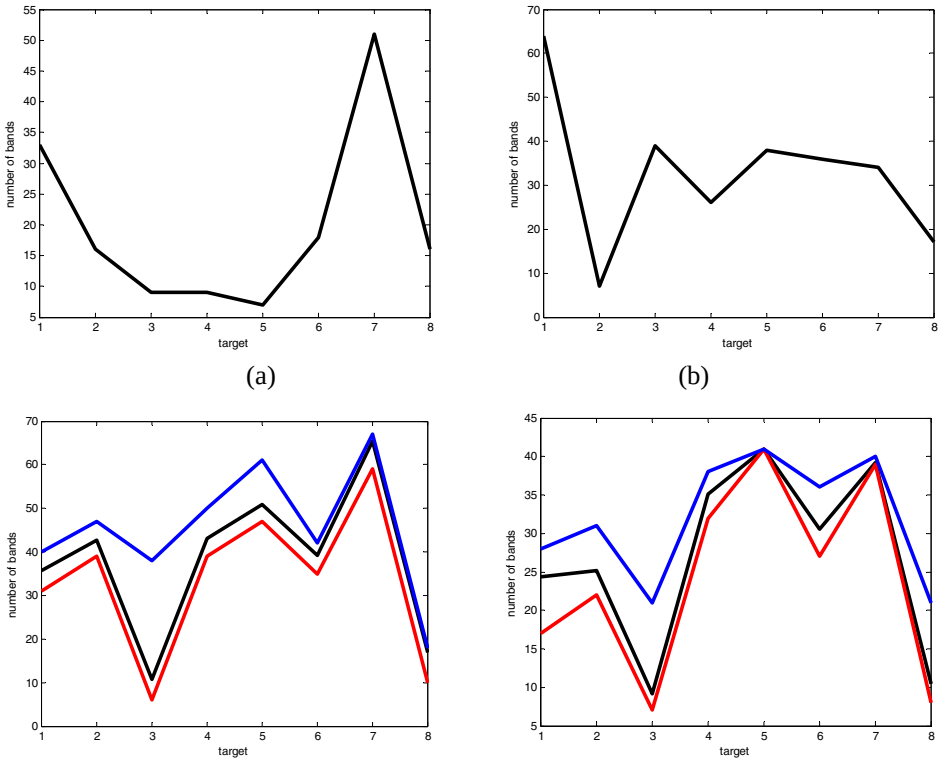

Figure 6. Number of bands resulting from the band screening for a) SBMinT-SA, b) SBMinT-SID, c) SBMaxBT-SA, d) SBMaxBT-SID.

We applied the six algorithms to the data with each of the average target spectra. Since regular spectral screening does not result in a unique set, to ensure a better uniformity we permuted the original data spectra prior to screening. The tests were performed on 10 different permutations. Fig. 6 displays the number bands resulting for each target after the band screening. We note that, depending on the nature of the target this number could vary significantly. Fig. 6 c. and d. also display the minimum and maximum number of bands, since in the case of SBMaxBT the algorithm is dependent on the random background pixels that are used. In our case, the background is formed of 200 random pixels from which we have excluded (if necessary) the target pixels.

For succinctness, we display the resulting detection images only from MSS-SA (see Fig. 7) with the mention that most of the other runs yielded similar results. Figs 8 display the detection graphs for α 0.1, and 0.5 respectively. At small thresholds such as 0.5, most of the pixels are classified as targets. With the exception of the fourth target, approximately 50% of the pixels are considered targets with no significant difference in quality noticed among the methods. A significantly different situation is noticed for α = 0.5. In this case, band screening seems to lead to an increase in false detection when compared to regular spectral screening algorithms. We note that both MSS-SID and MSS-SA follow the same graph pattern. While the results seem to suggest that band screening may not improve accuracy in target detection, we note that all most of the band selection methods were able to better classify target 7 than MSS. We also note that an increase in accuracy is expected when the number of background samples and target spectra is increased. In our experiments, given only four target spectra, we believe that the within class variability is rather limited.

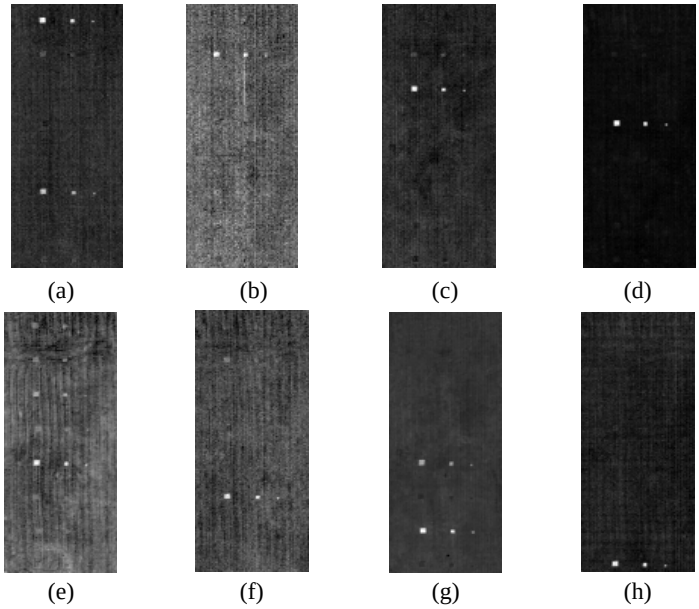

Figure 7. Classification images using Max SS-SA-OSP target detection

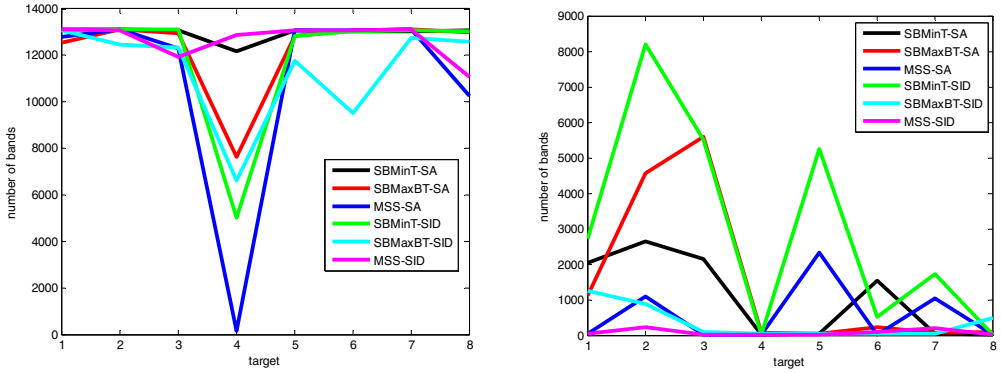

Figure 8. Detection graphs for the six methods thresholds a)0.1 b)0.5

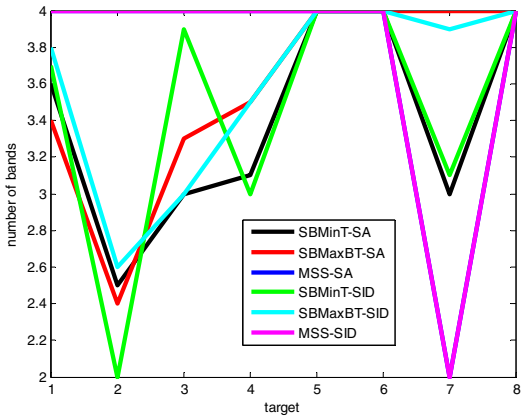

Figure 9. Detection graphs for the six methods when only the four target spectra are considered. The threshold value is 0.1

CONCLUSIONS

We presented a hybrid class of methods for target detection based on *band and spectra separability*. The unsupervised algorithms generate first a set of bands that increase the separability of the target from the background. Next, with the target spectra as origin, the algorithms generate a set of spectra that are dissimilar from each other in terms of a spectral distance measure. The spectral subset is obtained through Maximum spectral screening, a modified spectral selection algorithm. While spectral screening, the subset is built gradually with each newly added spectra being dissimilar from the ones already selected, in MSS the next spectra is always the most dissimilar one.

If we eliminate from the subset the desired target spectra we end up with a collection of signatures that characterize the background (with respect to the spectra). The spectral subset is thus used to build a target detection filter that, using orthogonal subspace projection will identify pixels that closely match the selected spectra. The developed algorithms were tested on HYDICE hyperspectral data using the spectral angle and the spectral information divergence. The results indicate that regular MSS outperforms band selection followed by MSS. Nevertheless, future studies are warranted in understanding how background sample size and target spectra population size influence the accuracy of the results.

ACKNOLWDGEMENT

The project was supported by a 2006-2009 FSP release award from Montclair State University.

REFERENCES

Achalakul T., and S. Taylor (2003), "A distributed spectral-screening PCT algorithm", *Journal of Parallel and Distributed Computing*, **63**, no. 3, 373-384.

Bannon D., and D. Milner (2004), "Information Across the Spectrum", Oemagazine, no. 3, 18-20.

Bowles, J. H., Antoniades, J. A., Baumback, M. M., Grossmann, J. M., Haas, D., Palmadesso, P. J., and J., Stracka (1997), Real-time analysis of hyperspectral data sets using NRL's ORASIS algorithm, *Proceedings SPIE Imaging Spectrometry III*, 3118,38-45.

Bowles, J., Chen, W., and D., Gillis (2003), "ORASIS framework – benefits to working within the linear mixing model", *Proceedings Igarss03*, 96-98.

Carvalho O.A. de, and P.R. Meneses (2000), "Spectral Correlation Mapper (SCM): An Improvement on the Spectral Angle Mapper (SAM)", NASA JPL AVIRIS Workshop.

Chang C.-I.,(2000), ''An information theoretic-based approach to spectral variability, similarity and discriminability for hyperspectral image analysis,'' *IEEE Transactions on Information Theory* **46**, no 5, 1927–1932.

Du H., Chang C.-I., Ren H., Chang C-C, Jensen J. O., and F. M. D'Amico (2004) "New hyperspectral discrimination measure for spectral characterization", *Optical Engineering*, 43(8): 1777–1786.

Harsanyi J.C., and C.-I. Chang, (1994), "Hyperspectral image classification and dimensionality reduction: An orthogonal subspace projection", *IEEE Transactions on Geoscience and Remote Sensing*, **32**, 779-785.

Hydice (1995), *Hyperspectral Digital Imagery Collection Experiment Documentation.*

Intel Inc., (2007), *Teraflops Research Chip,* http://www.intel.com/research/platform/terascale/teraflops.htm, (accessed February 15, 2007).

Keshava N., (2004), "Distance metrics and band selection in hyperspectral processing with applications to material identification and spectral libraries", *IEEE Trans. Geosci. Remote Sensing*, 2004, vol. 42, no.7, 1552- 1565.

Kruse F.A, Lekoff A.B., Boardman J.W., Heidebrecht K.B., Shapiro A.T., Barloon P.J., and A.F.H. Goetz (1993), "The Spectral Image Processing System (SIPS) – interactive visualization and analysis of imaging spectometer data", Remote Sensing of the Environment, 44, 145-163.

Kwon H., N. M. Nasrabadi (2006), "Kernel matched subspace detectors for hyperspectral target detection," IEEE Trans. Pattern Analysis and Machine Learning, vol. 28, pp. 178-194.

Lillesand, T. M. and R.W. Kiefer (2000). *Remote sensing and image interpretation*, John Wiley and Sons, New York.

Plaza A., Martínez P., Pérez R., and J Plaza, (2004) "A Quantitative and Comparative Analysis of Endmember Extraction Algorithms From Hyperspectral Data", *IEEE Trans. Geosci. Remote Sensing*, vol. 42, no. 3, 650-663.

Ren H., and C.-I. Chang, (2000a), "A Generalized Orthogonal Subspace Projection Approach to Unsupervised Multispectral Image Classification", *IEEE Transactions on Geosciences and Remote Sensing*, **38**, no. 6, 2515-2528.

Ren H., and C.-I. Chang, (2000b), "An experiment-based quantitative and comparative analysis of hyperspectral target detection and image classification algorithms", *IEEE Transactions on Geoscience and Remote Sensing*, **38**, 1044-1063.

Ren H., and C.-I. Chang, (2003), "Automatic Spectral Target Recognition in Hyperspectral Imagery", *IEEE Transactions on Aerospace and Electronic Systems*, **39**, no. 4, 1232-1249.

Richards, J. A. and X. Jia (1999). *Remote Sensing Digital Image Analysis*, Springer, New York.

Robila S.A., (2003), "Investigation of Spectral Screening Techniques for Independent Component Analysis Based Hyperspectral Image Processing", *SPIE Algorithms and Technologies for Multispectral, Hyperspectral, and Ultraspectral Imagery IX*, vol. 5093, 241-252.

Robila, S. A. (2005a), "Using Spectral Distances for Speedup in Hyperspectral Image Processing", *International Journal of Remote Sensing*, vol 26, no. 24, pp. 5629-5650.

Robila, S. A., and A. Gershman (2005b), "Spectral Matching Accuracy in Processing Hyperspectral Data", Proceedings*IEEE ISSCS,* ( ): 163-166.

Robila S.A., (2006), "A Maximum Spectral Screening (MSS) algorithm for target detection", in C.-I. Chang (ed.), *Recent Advances in Hyperspectral Signal and Image Processing*, Transworld Research Network, 297-326.